Arch. Pharm. Res.
DOI 10.1007/s12272-016-0882-x

RESEARCH ARTICLE

Synthesis and anti-mycobacterial activity of 4-(4-phenyl-1*H*-1,2,3-triazol-1-yl)salicylhydrazones: revitalizing an old drug

Hajjaj H. M. Abdu-Allah[1] · Bahaa G. M. Youssif[1,2] · Mostafa H. Abdelrahman[3] · Mohammed K. Abdel-Hamid[4] · Rudraraju Srilakshmi Reshma[5] · Perumal Yogeeswari[5] · Tarek Aboul-Fadl[4] · Dharmarajan Sriram[5]

Received: 13 August 2016 / Accepted: 22 December 2016

Abstract The antitubercular drug; *para*-aminosalicylic acid (PAS) was used as the core scaffold for the design of a series of 1*H*-1,2,3-triazolylsalicylhydrazones upon coupling with triazole and arylhydrazone moietis to furnish a single molecular architecture. The obtained derivatives were screened against *Mycobacterium tuberculosis* H37Rv revealing good to high activity for the active compounds (MIC values of 0.39–1.5 μg/mL) compared to the marketed drugs isoniazid, rifampicin and ethambutol. Moreover, the most active analogue *N*-(1-(4-chlorobenzyl)-2-oxoindolin-3-ylidene)-2-hydroxy-4-(4-phenyl-1*H*-1,2,3-triazol-1-yl)-benzohydrazide (**20**) was found to be ten-fold more potent than PAS and equipotent to rifampicin (MIC 0.39 μg/mL), while exhibiting low cytotoxicity with a selectivity index of >128. In addition, this compound was shown to be active against persistent forms of mycobacteria comparable to standard drugs in nutrient starvation model. Accordingly, we introduce compound **20** as a valuable lead for further development. A 3D-QSAR study was also conducted to help in explaining the observed activity and to serve as a tool for further development.

Keywords Antitubercular · *p*-Aminosalicylic · Dormant TB · Triazole · Isatin · Hydazide and modeling

Electronic supplementary material The online version of this article (doi:10.1007/s12272-016-0882-x) contains supplementary material, which is available to authorized users.

✉ Hajjaj H. M. Abdu-Allah
hagag.abdallah@pharm.au.edu.eg

✉ Dharmarajan Sriram
dsriram@hyderabad.bits-pilani.ac.in

1 Pharmaceutical Organic Chemistry Department, Faculty of Pharmacy, Assiut University, Assiut 71526, Egypt

2 Department of Pharmaceutical Chemistry, College of Pharmacy, Aljouf University, Aljouf, Sakaka 42421, Saudi Arabia

3 Department of Organic Chemistry, Faculty of Pharmacy, Al-Azhar University, Assiut 71524, Egypt

4 Medicinal Chemistry Department, Faculty of Pharmacy, Assiut University, Assiut 71526, Egypt

5 Medicinal Chemistry and Antimycobacterial Research Laboratory, Pharmacy Group, Birla Institute of Technology & Science-Pilani, Hyderabad Campus, Jawahar Nagar, Hyderabad, Telangana 500078, India

Introduction

Tuberculosis (TB), one of the most refractory and deadly infectious diseases worldwide, is a chronic bacterial infection caused by *Mycobacterium tuberculosis* (MTB). According to the WHO, nearly one third of the population is infected with tuberculosis that kills nearly 1.4 million people each year (WHO 2015). Most infections in human result in asymptomatic, latent infection and about one in ten latent infections eventually progresses to active disease (WHO 2015). The situation is more complicated by the emergence of multidrug resistant (MDR-TB) and extensively drug resistant (XDR-TB) strains. Therefore, the discovery of new drugs with different modes of action and toxicity profiles is urgently needed for use in the global effort to combat and eradicate the disease (Zumla et al. 2013). A common approach in drug design is the use of so-called privileged structures, which refers to substructures or scaffolds that appear frequently in drugs, natural products, or bioactive molecules (Evans et al. 1988; Verma et al. 2013). One of those privileged frameworks is the aminosalicylate moiety which has been shown in various drug classes that exhibit a broad range of applications such

Published online: 27 December 2016

as anticancer, antioxidant, antibacterial, and neuroprotective activity (Abdu-Allah et al. 2016a). In particular, *para*-aminosalicylic acid (PAS) which entered the clinical market as antitubercular agent in 1946 as the second exclusive drug after streptomycin (Minato et al. 2015). While PAS was initially a first-line treatment TB drug, the introduction of more potent antitubercular agents relegated PAS to the second line of treatment of drug-resistant *Mycobacterium tuberculosis* infections. The reported molecular and biochemical mechanisms involve PAS-mediated disruption of iron acquisition and corrupting one-carbon metabolism through inhibition of the formation of reduced folate species (Minato et al. 2015). Due to the short serum half-life of PAS, large oral doses (10–12 g per day) are required which result in a wide range of adverse effects, such as gastrointestinal symptoms, hypersensitivity reactions, and renal failure (Humma 1996; Peloquin et al. 1999). While it has been more than ten years since the synthesis of the last reported PAS antitubercular (Rengarajan et al. 2004; Patole et al. 2006), it would be necessary to revisit this molecule aiming for the production of new analogues that may be effective against existing PAS-resistant strains. On the other hand, different families of compounds have been reported with antitubercular activities such as hydrazones (Vavříková et al. 2011, Pavan et al. 2010) and isatins (Aboul-Fadl et al. 2010, 2011, Sriram et al. 2006). Investigation of SAR of isatin derivatives has revealed that 5-halogenation and *N*-alkylation have resulted in marked increase in antitubercular activity (Aboul-Fadl et al. 2010, 2011, Sriram et al. 2006). Moreover, triazoles have recently received much attention as central core in the synthesis of antitubercular agents (Emmadi et al. 2015; Suman et al. 2015; Menendez et al. 2012; Shanmugavelan et al. 2011; Jordão et al. 2011). In continue of our interest in the development of antitubercular agents (Aboul-Fadl et al. 2010, 2011, Sriram et al. 2006) and synthesis and biological activities of aminosalicylate derivatives (Abdu-Allah et al. 2005, 2016b; Abdel-Alim et al. 2005), the present work describes the synthesis and biological evaluation of a series of 1*H*-1,2,3-triazolylsalicylhydrazones starting from PAS as an attempt to its revitalization as antitubercular drug. The designed compounds **3**–**21** combine the core fragments of PAS, triazole and hydrazones in a single molecular architecture with the aim of improving the spectrum, potency and safety (Fig. 1).

Materials and methods

All chemicals and solvents were obtained from commercial suppliers and used without further purification. The starting material ethyl 4-azido-2-hydroxybenzoate, compound **1** was prepared according to the reported method (Gano et al. 2001). Melting points were determined on an electro thermal melting point apparatus [Stuart Scientific, model SMP3, England, UK], and were uncorrected. Pre-coated silica gel plates (kieselgel 0.25 mm, 60G F254, Merck, Germany) were used for TLC monitoring of reactions. The spots were detected at 254 nm wavelength using ultraviolet lamp (Spectroline, model CM-10, USA). IR spectra (KBr discs) were recorded on a shimadzu IR-470 spectrometer (Shimadzu, Kyoto, Japan) at Faculty of Pharmacy, Assiut University, Assiut, Egypt. NMR Spectra were taken using a Varian Unity INOVA 400 MHz spectrometer for proton and carbon at 400 and 100 MHz, respectively, University of Aberdeen, Aberdeen, UK. High resolution mass spectrometric data were obtained using the EPSRC mass spectrometry center in Swansea (UK) on a LTQ Orbitrap XL instrument.

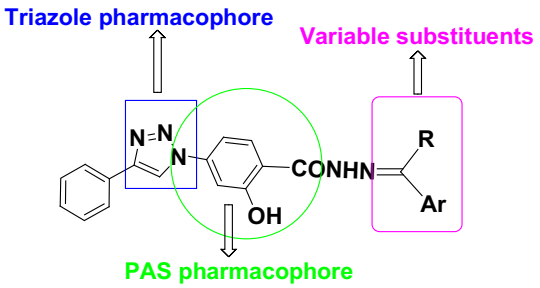

Fig. 1 Design strategy for the synthesis of triazolylsalicylhydrazones (**4**–**21**)

Synthesis of ethyl 2-hydroxy-4-(4-phenyl-1*H*-1,2,3-triazol-1-yl)-benzoate (2)

To a solution of compound **1** (4.14 g, 20.0 mmol) in a mixture of THF/H_2O [2:1 (v/v), 30 mL], phenyl acetylene (2.44 g, 24.0 mmol), $CuSO_4.5H_2O$ (0.24 g, 1.0 mmol) and sodium ascorbate (0.40 g, 2.0 mmol) were added. The mixture was stirred at room temperature for 20 h. the residue was extracted with $CHCl_3$ (3 × 15 mL), the organic phase was washed with water, dried over anhydrous Na_2SO_4 and concentrated. The crude product was crystallized from ethanol to afford pure compound as a white solid in 86% yield. m.p. 162–163 °C; IR (KBr): 3390, 3125, 3034, 2914, 1660, 1594, 1503, 1466, 1406, 1231, 874, 771, 688 cm^{-1}; ^1H NMR (DMSO-d6): δ (ppm): 10.91 (s, 1H); 9.40 (s, 1H); 7.95 (t, 2H, $J = 9.5$ Hz); 7.96–7.23 (m, 6H); 4.50–4.24 (q, 2H, $J = 8.2$ Hz); 1.34 (t, 3H, $J = 8$ Hz,); ^{13}C NMR (DMSO-d6): δ (ppm): 167.86; 160.92; 147.44; 141.09; 131.87; 131.54; 129.83; 128.86; 128.26; 125.24; 119.47; 112.93; 110.24; 107.60; 61.48; 13.85.

Synthesis of 2-hydroxy-4-(4-phenyl-1*H*-1,2,3-triazol-1-yl)-benzohydrazide (3)

To a solution of ethyl 2-hydroxy-4-(4-phenyl-1*H*-1,2,3-triazol-1-yl)benzoate (**2**) (3.09 g, 10.0 mmol) in absolute ethanol (40 mL), hydrazine hydrate 99% (0.75 g, 15.0 mmol) was added. The reaction mixture was refluxed for 6 h, and then cooled. The precipitated product was filtered, washed with cold ethanol, dried, and crystallized from ethanol as white crystals in 85% yield. m.p. 295–297 °C; IR (KBr): 3335, 3278, 1620, 1583, 1525, 1448, 1335, 1252, 933, 847, 748 cm^{-1}; ^1H NMR (DMSO-d6): δ (ppm): 10.33 (s, 1H); 9.35 (s, 1H); 8.05 (d, 1H, $J = 8.5$ Hz,); 7.98–7.90 (m, 2H); 7.56–7.44 (m, 4H); 7.41–7.34 (m, 1H); ^{13}C NMR (DMSO-d6): δ (ppm): 160.71; 147.44; 139.72; 130.05; 129.06; 128.36; 125.38; 119.57; 114.59; 109.73; 107.86; HRESI-MS m/z calcd for $C_{15}H_{13}N_5O_2$ $[M+H]^+$ 296.1142 Found 296.1134.

Synthesis of compounds (4–21)

To a suspension 2-hydroxy-4-(4-phenyl-1*H*-1,2,3-triazol-1-yl)benzohydrazide **(3)** (0.29 g, 1.0 mmol) in ethanol (10 mL) and the appropriate aryl carbonyl compound (1.0 mmol), 2 drops of glacial acetic acid were added, then the reaction mixture was heated under reflux for 6 h. The reaction mixture was cooled and the precipitated product was filtered, washed with cold ether and recrystallized from aqueous DMF to give yellow solid product.

*N^1-(4-(Dimethylamino)benzylidene)-2-hydroxy-4-(phenyl-1H-1,2,3-triazol-1-yl)- benzohydrazide (**4**)*

Yield 57%, m.p 293–294 °C; IR (KBr): 3424, 3287, 3134, 2914, 1651, 1614, 1593, 1533, 1350, 1314, 1234 1188, 845, 766 cm^{-1}; ^1H NMR (DMSO-d6): δ (ppm): 12.67 (s, 1H); 11.73 (s, 1H); 9.38 (s, 1H); 8.33 (s, 1H); 8.14 (d, 1H, $J = 8.4$ Hz); 7.96 (d, 2H, $J = 7.7$ Hz); 7.54 (dt, 6H, $J = 30.2$, 7.6 Hz); 7.39 (t, 1H, $J = 7.5$ Hz); 6.75 (d, 2H, $J = 8.4$ Hz); 2.97 (s, 6H); ^{13}C NMR (DMSO-d6): δ (ppm): 163.63; 160.52; 151.71; 150.13; 147.49; 139.86; 130.06; 130.03; 129.02; 128.75; 128.38; 125.39; 121.10; 119.75; 115.65; 111.74; 109.84; 107.83; 39.73; HRESI-MS *m/z* calcd for $C_{24}H_{22}N_6O_2$ $[M+H]^+$ 427.1877 Found 427.1863.

*N^1-(3-Bromobenzylidene)-2-hydroxy-4-(4-phenyl-1H-1,2,3-triazol-1-yl)-benzohydrazide (**5**)*

Yield 71%, m.p. >300 °C; IR (KBr): 3450, 3255, 3035, 1639, 1617, 1551, 1515, 1253, 1042, 755, 795 cm^{-1}; ^1H NMR (DMSO-d6): δ (ppm): 12.31 (s, 1H); 12.03 (s, 1H); 9.38 (s, 1H); 8.44 (s, 1H); 8.11 (d, 1H, $J = 8.6$ Hz); 7.95 (d, 3H, $J = 7.7$ Hz); 7.75 (d, 1H, $J = 7.7$ Hz); 7.60 (dt, 3H, $J = 20.7$, 5.5 Hz); 7.50 (t, 2H, $J = 7.7$ Hz); 7.41 (dt, 2H, $J = 15.0$, 7.6 Hz); ^{13}C NMR (DMSO-d6): δ (ppm): 163.85; 159.87; 147.51; 140.01; 136.50; 132.84; 131.02; 130.71; 130.00; 129.01; 128.38; 126.39; 125.40; 122.19; 119.59; 116.21; 110.04; 107.87; HRESI-MS *m/z* calcd for $C_{22}H_{16}BrN_5O_2$ $[M+H]^+$ 462.0560 Found 462.0550.

*N^1-(3-Chlorobenzylidene)-2-hydroxy-4-(4-phenyl-1H-1,2,3-triazol-1-yl)-benzohydrazide (**6**)*

Yield 71%, m.p. 301–302 °C; IR (KBr): 3327, 3275, 3129, 1661, 1616, 1590, 1549, 1517, 1411, 1347, 1238, 1155, 1076, 779, 686 cm^{-1}; ^1H NMR (DMSO-d6): δ (ppm): 12.33 (s, 1H); 12.02 (s, 1H); 9.37 (s, 1H); 8.45 (s, 1H); 8.11 (d, 1H, $J = 8.6$ Hz); 7.95 (d, 2H, $J = 7.6$ Hz); 7.79 (s, 1H); 7.71 (t, 1H, $J = 4.4$ Hz); 7.65–7.56 (m, 2H); 7.56–7.45 (m, 5H); 7.38 (t, 1H, $J = 7.4$ Hz); ^{13}C NMR (DMSO-d6): δ (ppm): 163.88; 159.92; 147.51; 147.26; 140.02; 136.27; 133.69; 130.74; 130.68; 130.01; 129.96; 129.00; 128.37; 126.50; 125.97; 125.40; 119.57; 116.14; 110.02; 107.78; HRESI-MS *m/z* calcd for $C_{22}H_{16}ClN_5O_2$ $[M+H]^+$ 418.1065 Found 418.1051.

*N^1-(4-Fluorobenzylidene)-2-hydroxy-4-(4-phenyl-1H-1,2,3-triazol-1-yl)-benzohydrazide (**7**)*

Yield 47%, m.p. >300 °C; IR (KBr): 3420, 3267, 3086, 1624, 1559, 1508, 1407, 1236, 1152, 1040, 925, 833, 788, 764, 691 cm^{-1}; ^1H NMR (DMSO-d6): δ (ppm): 12.39 (s, 1H); 11.97 (s, 1H); 9.38 (d, 1H, $J = 3.6$ Hz); 8.47 (d, 1H, $J = 3.5$ Hz); 8.12 (dd, 1H, $J = 8.6$, 3.6 Hz); 7.95 (dd, 2H, $J = 7.7$, 3.6 Hz); 7.81 (ddd, 2H, $J = 8.8$, 5.5, 3.0 Hz); 7.65–7.53 (m, 2H); 7.49 (td, 2H, $J = 7.6$, 3.5 Hz); 7.38 (td, 1H, $J = 7.5$, 3.6 Hz); 7.30 (td, 2H, $J = 8.7$, 3.5 Hz); ^{13}C NMR (DMSO-d6): δ (ppm): 164.52; 163.83; 162.05; 160.14; 147.87; 147.50; 139.98; 130.67; 130.56; 130.02 129.54; 129.46; 129.01; 128.37; 125.39; 119.58; 116.07; 115.85; 109.92; 107.84; HRESI-MS *m/z* calcd for $C_{22}H_{16}FN_5O_2$ $[M+H]^+$ 402.1361 Found 402.1350.

*N^1-(4-Chlorobenzylidene)-2-hydroxy-4-(4-phenyl-1H-1,2,3-triazol-1-yl)-benzohydrazide (**8**)*

Yield 86%, m.p. 300–301 °C; IR (KBr): 3423, 3274, 3064, 1620, 1548, 1515, 1490, 1405, 1237, 1090, 923, 823, 763, 690, 627 cm^{-1}; ^1H NMR (DMSO-d6): δ (ppm): 12.04 (s, 1H); 11.95 (s, 1H); 9.14 (d, 1H, $J = 3.6$ Hz); 8.50 (d, 1H, $J = 3.5$ Hz); 7.96 (br. d, 1H); 7.81 (dd, 2H, $J = 7.5$, 3.4 Hz); 7.52–7.43 (m, 9H); ^{13}C NMR (DMSO-d6): δ (ppm): 164.52; 163.83; 162.05; 160.14; 147.9; 147.50; 139.98; 130.30; 130.56; 130.02 129.40; 129.46; 129.01; 128.8; 120.4; 119.58; 116.07; 115.85; 109.92; 107.84;

HRESI-MS *m/z* calcd for $C_{22}H_{16}ClN_5O_2$ $[M+H]^+$ 418.1071 Found 418.1000.

*2-Hydroxy-N^1-(2-hydroxybenzylidene)-4-(4-phenyl-1H-1,2,3-triazol-1-yl)-benzohydrazide (**9**)*

Yield 65%, m.p. >300 °C; IR (KBr): 3440, 3260, 3064, 1636, 1620, 1546, 1516, 1466, 1406, 1361, 1237, 1037, 863, 752, 690 cm^{-1}; ^1H NMR (DMSO-d6): δ (ppm): 12.15 (s, 1H); 11.16 (s, 1H); 9.38 (s, 1H); 8.71 (s, 1H); 8.13 (d, 1H, $J = 8.2$ Hz); 7.95 (d, 2H, $J = 7.4$ Hz); 7.70–7.26 (m, 9H); 6.94 (t, 2H, $J = 6.8$ Hz); ^{13}C NMR (DMSO-d6): δ (ppm): 157.47; 147.48; 131.70; 129.96; 129.00; 128.38; 125.36; 119.60; 119.40; 116.43; 110.06; HRESI-MS *m/z* calcd for $C_{22}H_{17}N_5O_3$ $[M+H]^+$ 400.1404 Found 400.1395.

*N^1-(2,6-Dichlorobenzylidene)-2-hydroxy-4-(4-phenyl-1H-1,2,3-triazol-1-yl)-benzohydrazide (**10**)*

Yield 97%, m.p. 279–280 °C; IR (KBr): 3421, 3282, 3128, 3066, 1678, 1616, 1579, 1546, 1413, 1237, 1158, 1066, 931, 765, 688 cm^{-1}; ^1H NMR (DMSO-d6): δ (ppm): 12.21 (s, 1H); 9.40 (s, 1H); 8.70 (s, 1H); 8.13 (d, 1H, $J = 8.5$ Hz); 7.96 (d, 2H, $J = 7.8$ Hz); 7.65–737 (m, 10H); ^{13}C NMR (DMSO-d6): δ (ppm): 164.15; 160.06; 147.52; 144.39; 140.10; 134.01; 131.38; 130.67; 130.35; 130.01; 129.13; 129.02; 128.39; 125.40; 119.63; 116.10; 110.04; 109.55; 107.83; HRESI-MS *m/z* calcd for $C_{22}H_{15}Cl_2N_5O_2$ $[M+H]^+$ 452.0676 Found 452.0662.

*N^1-(Benzo[d][1,3]dioxol-5-ylmethylene)-2-hydroxy-4-(4-phenyl-1H-1,2,3-triazol-1-yl)-benzohydrazide (**11**)*

Yield 87%, ^1H NMR (DMSO-d6): δ (ppm): 12.44 (s, 1H); 11.87 (s, 1H); 9.38 (s, 1H); 8.12 (s, 1H); 7.95 (d, 2H, $J = 7.2$ Hz); 7.64–7.55 (m, 2H); 7.50 (t, 3H, $J = 7.4$ Hz); 7.39 (t, 1H); 7.33 (s, 1H); 7.21 (d, 1H, $J = 7.6$ Hz); 7.00 (d, 1H, $J = 7.4$ Hz); 6.1 (s, 2H); ^{13}C NMR (DMSO-d6): δ (ppm): 160.23; 149.39; 148.91; 148.03; 147.51; 139.95; 130.39; 130.02; 129.02; 128.39; 125.40; 123.75; 119.58; 109.94; 108.51; 105.26; 101.65; HRESI-MS *m/z* calcd for $C_{23}H_{17}N_5O_4$ $[M+H]^+$ 428.1353 Found 428.1340.

*N^1-(2,5-Dimethoxybenzylidene)-2-hydroxy-4-(4-phenyl-1H-1,2,3-triazol-1-yl)-benzohydrazide (**12**)*

Yield 90%, m.p. 277–278 °C; IR (KBr): 3459, 3265, 3080, 2943, 2835, 1662, 1610, 1548, 1516, 1495, 1466, 1263, 1263, 1041, 938, 764, 709 cm^{-1}; ^1H NMR (DMSO-d6): δ (ppm): 12.04 (s, 1H); 11.23 (s, 1H); 9.38 (s, 1H); 8.12 (s, 1H); 7.95 (d, 2H, $J = 7.2$ Hz); 7.64–7.55 (m, 2H); 7.50 (t, 3H, $J = 7.4$ Hz); 7.39 (t, 1H,); 7.33 (s, 1H); 7.21 (d, 1H, $J = 7.6$ Hz); 7.00 (d, 1H, $J = 7.4$ Hz); 6.1 (br.s, 2H); 3.85 (s, 6H); ^{13}C NMR (DMSO-d6): δ (ppm): 160.23; 149.39; 148.91; 148.03; 147.51; 139.95; 130.39; 130.02; 129.02; 128.39; 125.40; 123.75; 119.58; 109.94; 108.51; 105.26; 101.65; 65.00; HRESI-MS *m/z* calcd for $C_{24}H_{22}N_5O_4$ $[M+H]^+$ 444.1666 found 444.1649.

*2-Hydroxy-4-(4-phenyl-1H-1,2,3-triazol-1-yl)-N^1-(pyridine-2-ylmethylene)-benzohydrazide (**13**)*

Yield 78%, m.p. 287–288 °C; IR (KBr): 3435, 3263, 3137, 3052, 1635, 1618, 1552, 1467, 1237, 1040, 940, 778, 742, 629 cm^{-1}; ^1H NMR (DMSO-d6): δ (ppm): 12.12 (s, 1H); 9.38 (s, 1H); 8.63 (d, 1H, $J = 4.6$ Hz); 8.50 (s, 1H); 8.20-7.85 (m, 7H); 7.66–7.34 (m, 9H); ^{13}C NMR (DMSO-d6): δ (ppm): 164.14; 160.02; 152.99; 149.57; 149.08; 147.52; 140.05; 136.89; 130.63; 130.02 128.36; 125.41; 124.59; 120.17; 119.58; 116.23; 109.99; 107.79; HRESI-MS *m/z* calcd for $C_{21}H_{16}N_6O_2$ $[M+H]^+$ 385.1408 Found 385.1396.

*2-Hydroxy-4-(4-phenyl-1H-1,2,3-triazol-1-yl)-N^1-((z)-3-phenylallylidene)-benzohydrazide (**14**)*

Yield 83%, m.p. 284–285 °C; IR (KBr): 3438, 3280, 3058, 1625, 1609, 1581, 1518, 1245, 1142, 1077, 969, 915, 759, 690 cm^{-1}; ^1H NMR (DMSO-d6): δ (ppm): 12.43 (s, 1H); 11.85 (s, 1H); 9.39 (s, 1H); 8.27 (d, 1H, $J = 6.3$ Hz); 8.11 (d, 1H, $J = 8.6$ Hz); 7.96 (d, 2H, $J = 7.6$ Hz); 7.71–7.30 (m, 13H); 7.10 (d, 2H, $J = 5.3$ Hz); ^{13}C NMR (DMSO-d6): δ (ppm): 163.81; 160.15; 151.09; 147.50; 140.02; 139.96; 135.78; 130.48; 130.01; 129.02; 128.85; 128.39; 127.22; 125.40; 125.34; 119.61; 116.00; 109.96; 107.80; HRESI-MS *m/z* calcd for $C_{24}H_{20}N_5O_2$ $[M+H]^+$ 410.1612 Found 410.1602.

*N^1-(1-(2-Fluorophenyl)ethylidene)-2-hydroxy-4-(4-phenyl-1H-1,2,3-triazol-1-yl)-benzohydrazide (**15**)*

Yield 75%, m.p. 281–282 °C; IR (KBr): 3439, 3318, 3137, 3075, 1674, 1614, 1519, 1257, 915, 753 cm^{-1}; ^1H NMR (DMSO-d6): δ (ppm): 11.37 (s, 1H); 9.37 (s, 1H); 9.30 (s, 1H); 8.19 (dd, 2H, $J = 19.9$, 8.5 Hz); 7.95 (dd, 3H, $J = 12.6$, 7.6 Hz); 7.72–7.23 (m, 16H); 2.32 (s, 3H); ^{13}C NMR (DMSO-d6): δ (ppm): 161.25; 158.77; 157.53, 156.69; 150.62; 147.53; 147.48; 139.73; 132.94; 132.59; 130.03; 129.99; 129.91; 129.00; 128.37; 125.62; 125.42; 125.39; 124.49; 124.46; 119.60; 119.55; 118.03; 116.26; 116.04; 110.69; 107.65; 107.45; 24.31; 17.21; 17.16; HRESI-MS *m/z* calcd for $C_{23}H_{18}FN_5O_2$ $[M+H]^+$ 416.1517 Found 416.1503.

*2-Hydroxy-N^1-(2-oxoindolin-3-ylidene)-4-(4-phenyl-1H-1,2,3-triazol-1-yl)-benzohydrazide (**16**)*

Yield 80%, m.p. >300 °C; IR (KBr): 3439, 3296, 3133, 1723, 1680, 1612, 1504, 1482, 1465, 1401, 1212, 1156,

1152, 1052, 757 cm^{-1}; ^1H NMR (DMSO-d6): δ (ppm): 12.44 (s, 1H); 11.17 (s, 1H); 9.36 (s, 1H); 8.22 (d, 1H, $J = 8.7$ Hz); 8.00–7.92 (m, 2H); 7.68 (d, 1H, $J = 2.1$ Hz); 7.63–7.32 (m, 2H); 7.09 (td, 1H, $J = 7.6$, 1.0 Hz); 6.93 (dt, 1H, $J = 7.7$, 0.9 Hz); 2.54 (s, 3H); HRESI-MS *m/z* calcd for $C_{23}H_{16}N_6O_3$ $[M+H]^+$ 425.1357 Found 425.1345.

*2-Hydroxy-N^1-(2-oxo-5-(trifluoromethoxy)indolin-3-ylidene)-4-(4-phenyl-1H-1,2,3-triazol-1-yl)-benzohydrazide (**17**)*

Yield 72%, m.p. >300 °C; IR (KBr): 3430, 3140, 3064, 1671, 1613, 1485, 1403, 1277, 1248, 1205, 1138, 1055, 929, 827, 675 cm^{-1}; ^1H NMR (DMSO-d6): δ (ppm): 11.35 (s, 1H); 9.36 (s, 1H); 8.23 (d, 1H, $J = 8.6$ Hz); 8.00-7.92 (m, 2H); 7.68 (d, $J = 2.1$ Hz, 1H); 7.56 (dd, 1H, $J = 8.7$, 2.1 Hz); 7.52–7.45 (m, 3H); 7.43–7.33 (m, 2H); 7.01 (d, 1H, $J = 8.5$ Hz); HRESI-MS *m/z* calcd for $C_{24}H_{15}F_3N_6O_4$ $[M+H]^+$ 509.1180 Found 509.1169.

*Sodium 3-(2-(2-hydroxy-4-(4-phenyl-1H-1,2,3-triazol-1-yl)benzoyl)hydrazono)-2-oxo- indoline-5-sulfonate (**18**)*

Yield 57%, m.p. >300 °C; IR (KBr): 3399, 3139, 3088, 1717, 1685, 1617, 1537, 1510, 1212, 1190, 1152, 1029, 726 cm^{-1}; ^1H NMR (DMSO-d6): δ (ppm): 12.03 (s, 1H); 10.60 (s, 1H); 8.97 (d, 2H, $J = 7.1$ Hz); 7.94 (s, 1H); 7.86 (d, 1H, $J = 8.6$ Hz); 7.58 (d, 3H, $J = 7.8$ Hz); 7.42–7.35 (m, 2H); 7.16 (dt, 6H, $J = 34.0$, 8.3 Hz,); 7.01 (d, 2H, $J = 7.3$ Hz); 6.56 (d, 1H, $J = 8.1$ Hz); ^{13}C NMR (DMSO-d6): δ (ppm): 165.27; 147.57; 147.49; 142.48; 140.42; 138.65; 133.21; 130.40; 130.04; 129.06; 128.42; 125.45; 125.41; 121.59; 119.63; 114.58; 110.60; 110.19; 109.88; 108.15; 107.85; 107.66; HRESI-MS *m/z* calcd for $C_{23}H_{15}N_6NaO_6S$ $[M+H]^+$ 527.0744 Found 528.07649.

*N^1-(5-Chloro-2-oxoindolin-3-ylidene)-2-hydroxy-4-(4-phenyl-1H-1,2,3-triazol-1-yl)-benzohydrazide (**19**)*

Yield 75%, m.p. >300 °C; IR (KBr): 3450, 3140, 3057, 1721, 1683, 1616, 1511, 1465, 1243, 1147, 1023, 817, 758 cm^{-1}; ^1H NMR (DMSO-d6): δ (ppm): 11.27 (s, 1H); 9.34 (d, 1H, $J = 7.5$ Hz); 8.21 (d, 1H, $J = 8.6$ Hz); 7.95 (d, 2H, $J = 7.4$ Hz); 7.69–7.63 (m, 1H); 7.58–7.45 (m, 4H); 7.38 (t, 2H, $J = 7.6$ Hz); 6.92 (d, 1H, $J = 8.4$ Hz); HRESI-MS *m/z* calcd for $C_{23}H_{15}ClN_6O_3$ $[M+H]^+$ 459.0967 Found 459.0954.

*N^1-(1-(4-Chlorobenzyl)-2-oxoindolin-3-ylidene)-2-hydroxy-4-(4-phenyl-1H-1,2,3-triazol-1-yl)-benzohydrazide (**20**)*

Yield 77%, m.p. 277–279 °C; 3482, 3140, 3069, 1701, 1672, 1613, 1490, 1467, 1356, 1222, 1142, 1016, 763 cm^{-1}; ^1H NMR (DMSO-d6): δ (ppm): 12.60 (s, 1H); 9.36 (s, 1H); 8.24 (d, 1H, $J = 8.6$ Hz); 7.96 (d, 2H, $J = 7.6$ Hz); 7.69–7.61 (m, 2H); 7.56 (d, 1H, $J = 8.7$ Hz); 7.49 (t, 2H, $J = 7.6$ Hz); 7.45–7.32 (m, 6H); 7.14 (t, 1H, $J = 7.6$ Hz); 7.04 (d, 1H, $J = 7.9$ Hz); 5.00 (s,2H); ^{13}C NMR (DMSO-d6): δ (ppm): 159.86, 157.65; 147.56; 142.51; 140.37; 134.98; 132.26; 131.30; 129.97; 129.32; 128.99; 128.71; 128.38; 125.43; 123.18; 120.76; 119.95; 119.60; 110.11; 107.42; HRESI-MS *m/z* calcd for $C_{30}H_{21}ClN_6O_3$ $[M+H]^+$ 549.1436 Found 549.1414.

*2-Hydroxy-N^1-(1-(3-methoxybenzyl)-2-oxoindolin-3-ylidene)-4-(4-phenyl-1H-1,2,3-triazol-1-yl)-benzohydrazide (**21**)*

Yield 73%, m.p. 286–287 °C; IR (KBr): 3402, 3214, 3128, 3067, 1702, 1670, 1614, 1489, 1466, 1357, 1241, 1143, 1018, 765 cm^{-1}; ^1H NMR (DMSO-d6): δ (ppm): 9.36 (s, 1H); 8.25 (d, 1H, $J = 8.6$ Hz); 8.00-7.90 (m, 3H); 7.69-7.62 (m, 2H); 7.53 (dt, 4H, $J = 24.2$, 8.0 Hz); 7.43–7.33 (m, 2H); 7.26 (t, 1H, $J = 7.9$ Hz); 7.14 (t, 1H, $J = 7.5$ Hz); 7.05 (d, 1H, $J = 7.9$ Hz); 7.01–6.90 (m, 2H); 6.86 (dd, 1H, $J = 8.3$, 2.5 Hz); 4.96 (d, 2H, $J = 6.5$ Hz); 3.72 (d, 3H, $J = 2.3$ Hz,); ^{13}C NMR (DMSO-d6): δ (ppm):160.58; 159.87; 159.51; 157.65; 147.58; 142.73; 140.39; 137.48; 133.62; 130.03; 129.98; 129.93; 129.14; 129.03; 128.40; 125.44; 125.38; 123.15; 120.74; 119.89; 119.63; 119.38; 117.42; 113.47; 112.73; 110.81; 110.25; 109.79; 107.84; 107.45; 55.09; HRESI-MS *m/z* calcd for $C_{31}H_{24}N_6O_4$ $[M+H]^+$ 545.1932 Found 545.1919.

Biological screening

Anti-mycobacterial activity: In-vitro MABA assay

The anti-mycobacterial activities of compounds **4–21** were evaluated against *M. tuberculosis* H37Rv using Microplate Alamar Blue assay (MABA) (Franzblau et al. 1998). Bacterial inoculi of *Mycobacterium tuberculosis* H37Rv were prepared from fresh LJ medium and re-suspended in Middlebrook 7H9 broth supplemented with 10% OADC (HiMedia Laboratories). This culture was grown at 37 °C until the turbidity matched with McFarland no.1 turbidity standard. The culture was diluted to 1:25 with media and 100 µL was used as an inoculum. Each drug stock solution was thawed and diluted in Middlebrook 7H9-OADC at four-fold the final highest concentration tested. Serial two fold dilutions of each drug were prepared directly in a sterile 96-well microtiter plate using 100µL Middlebrook 7H9-OADC. Each plate also contained wells containing MTB cultures without addition of the tested compounds and wells with only sterile medium as controls. Sterile

water was added to all outer wells to avoid evaporation during incubation. The plate was covered, sealed in plastic bags and incubated at 37 °C. MIC values were determined using MABA assay (Franzblau et al. 1998). After 5 days of incubation, 50 µL of 1:1 mixture of alamar blue solution (Sigma Aldrich) and sterile 10% tween 80 (Nice chemicals) were added to each well and the plate was re-incubated overnight (reading on 7th day). A change in color from blue (oxidized state) to pink (reduced) indicated growth of bacteria and the minimum inhibitory concentration (MIC) was defined as the lowest concentration of the compound that prevented this change in color.

Nutrient starvation model

Compounds showing promising MIC (≤1.5 µg/mL) were evaluated for their efficiency against dormant forms of bacteria by nutrient starvation model. MTB dormant culture was prepared using nutrient starvation method (Betts et al. 2002; De Man 1983). In nutrient starvation model, culture of MTB H37Rv grown in Middlebrook 7H9 medium supplemented with OADC (nutrient rich medium) was pelleted and washed twice with PBS (Phosphate Buffer Saline, obtained from HiMedia Laboratories). The pellet was suspended in PBS in sealed bottles and was incubated at 37 °C for 6 weeks. These cultures were treated with standard drugs like isoniazid, rifampicin and moxifloxacin along with the synthesized compounds for 7 days at a concentration of 10 µg/mL. The treated cell suspensions were diluted 10-fold up to 10—6 using Middlebrook 7H9 medium supplemented with OADC and 100 µl of each dilution were plated in 48 well plates in triplicates along with 900 µl of Middlebrook 7H9 medium (HiMedia Laboratories) supplemented with OADC (HiMedia Laboratories). The plates were incubated at 37 °C for 3–4 weeks the wells with visible bacterial growth were counted as positive. The bacterial count was determined by using standard statistical methods using MPN assay.

Evaluation of cytotoxicity

The cytotoxic activity was measured in vitro against Human Embryonic Kidney (HEK-293T) cells at 50 µg/mL concentration using 3-(4,5-dimethylthiazol-2-yl)-2,5-diphenyltetrazolium bromide (MTT) assay (Sykes et al. 2012; Bézivin et al. 2003). The cells were cultured in a flat bottomed 96-well plate till a density of 5×10^5 cells was reached and the test compounds were respectively added to each well. While the incubation was permitted at 37 °C, with 5% CO_2 and 95% O_2 atmosphere for 48 h before the cytotoxicity assessments. Just before 4 h of the end of the incubation, 10 µL of MTT reagent (10 mg mL−1) was added per well. Four hours later, the 96-well plate was centrifuged at 1200 rcf for about 3 min and the supernatants were removed, subsequently to each well 200 µL of DMSO was added. The absorbance was measured at a wavelength of 490 nm on Victor-3-microplate reader against the blank. Three replicate wells were done for each concentration of drug to minimize the error rate. The cytotoxicity of each compound was expressed as % inhibition. The selective activities of the compounds were determined by calculating the selectivity index (SI). SI was calculated by dividing 50 µg/mL by MIC. As Cytotoxicity is less than 50% at 50 µg/mL. All the values are mentioned by ">". Selectivity index (SI) = 50 µg/mL/MIC µg/mL.

Pharmacophore modeling

The pharmacophore model was generated using the HypoGen algorithm of Catalyst software as implemented in Discovery Studio 4.1 package (Debnath 2002). Compounds **3–21** were built de novo with standard options within the 2D/3D editor sketcher of the program. Conformational analysis was performed using the "BEST" option with a maximum of 250 conformers per molecule and a 20 kcal/mol energy threshold above the calculated global minimum. The inactivity spread, uncertainty, and spacing parameters were set to 1.5, 2, and 1.8, respectively, as proposed by Accelrys for training sets with narrower activity span than usual. The hydrogen-bond-acceptor (HBA) and -donor (HBD), hydrophobic (HYD), and aromatic ring (AR) chemical features were considered for hypothesis generation and no excluded volumes. Hypothesis selection was done by a cost analysis procedure (represented in bit units) based on three terms: weight cost, error cost (penalizes the deviation between the estimated activities of the training set and their experimentally determined values); and configuration cost (penalizes the complexity of the hypothesis, should not exceed a maximum value of 18). The error cost contributes the most in determining the overall cost of a hypothesis. In addition, the costs of the ideal hypothesis, the simplest possible hypothesis that fits the data with minimal cost (fixed cost), and the null hypothesis in which the error cost is high (null cost) are computed by the HypoGen module. Statistically significant hypotheses possess total costs close to the fixed cost and far away from the null cost values.

Results and discussion

Chemistry

The synthesis of the target compounds (**3–21**) was achieved starting from PAS (Scheme 1) by the following sequence of reactions: PAS was esterified, diazotized and treated

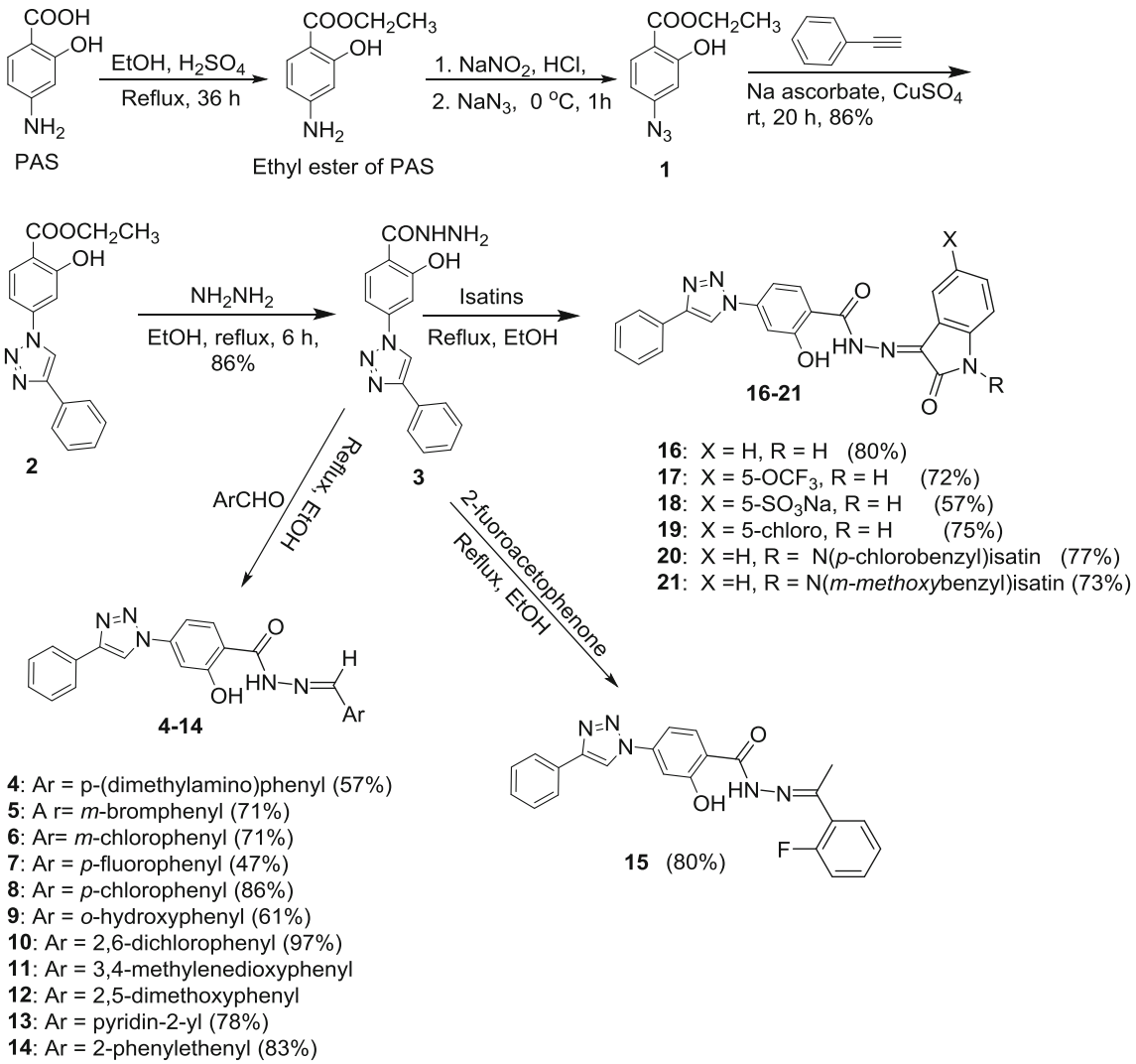

Scheme 1 Synthesis of the target compounds **3**–**21**

with sodium azide (Sandmyer reaction) to give ethyl 4-azidosalicylate **1** (Gano et al. 2001). This sequence of synthesizing **1** is critical for producing a solid easy to purify, while direct azidation of PAS produces a semisolid that was difficult to manipulate. Reacting **1** with phenylacetylene, using click chemistry, in presence of sodium ascorbate and copper sulfate in a mixture of THF/H_2O afforded a new intermediate ethyl 2-hydroxy-4-(4-phenyl-1*H*-1,2,3-triazol-1-yl)benzoate; compound **2.** The structure of **2** was confirmed by analyzing its ^{1}H NMR spectrum which shows the appearance of a triplet signal at δ 1.34 ppm and quartet at 4.50-4.24 ppm corresponding to C_2H_5 moiety, singlet 9.40 (-CH triazole) and singlet at 10.91 corresponding to OH group. The key intermediate *p*-(2-hydroxy-4-phenyl-1 *H*-1,2,3-triazol-1-yl)benzoichydrazide **3** was prepared by hydrazinolysis of **2** with hydrazine hydrate. IR spectrum of compound **(3)** showed bands at 3335, 3278 and 1620 cm^{-1} due to OH, $NHNH_2$ and C = O functions respectively, while it showed no signals derived from ethyl moiety in ^{1}H NMR spectrum. Finally, condensation of **3** with different aldehydes, *o*-fluoroacetophenone and isatins in ethanol gave the corresponding hydrazones **4**–**21**. IR, ^{1}H NMR, ^{13}C NMR and HRMS spectral data are in agreement with the proposed structures of the synthesized compounds. Hydrazones **4**–**21** show carbonyl amide stretching at about 1650 cm^{-1} and N–H bands in 3250–3200 cm^{-1} region. ^{1}H NMR spectra displayed additional signals due to the aromatic ring derived from aldehyde, acetophenone or isatin moieties in the aromatic region and showed two signals at about δ 7.35 ppm and δ 10.31 ppm which were attributed to the N–CH and NH protons, respectively. N = CH carbon of the compounds in the hydrazone structures were observed at δ 143.5–149.8 ppm in their ^{13}C NMR spectra.

The mass spectra of compounds showed [M+1] peaks in agreement with their molecular formula. The ^{1}H NMR

spectra of the derivatives **4–21** revealed only one N–H signal for each compound, which was attributed to the (*E*)-diastereomer, as reported for similar compounds (Jordão et al. 2011).

Anti-mycobacterial activity

The target compounds (**3–21**) were evaluated for their in vitro activity against *M. tuberculosis* H37Rv by MABA (Franzblau et al.1998). The MIC values (μg/mL) along with the standard drugs are presented in Table 1. Compounds **3–21** showed in vitro activity against MTB with MIC ranging from 0.39 to 25 μg/mL. Eight compounds (**4**, **5**, **7**, **10**, **12**, **13**, **19** and **20**) exhibited greater potency than PAS, while derivatives **4**, **5**, **12** and **20** exhibited higher potencies than ethambutol, and analogues **7**, **10**, **12**, **13**, **19** were equipotent to ethambutol. Interestingly, compound **20** (MIC 0.39 μg/mL) showed equipotent activity to rifampicin. A preliminary structure activity relationship was deduced based on the obtained biological activity. It was noted that the type of substituent on aromatic ring of the benzylidene group has a significant effect on the observed biological activity. Among the benzylidene derivatives, compounds **4** (*p*-N$(CH_3)_2$), **5** (*m*-Br) and **12** (2,5-diMeO) showed high potency (MIC 1.5 μg/mL). Accordingly, it seems that inductively electron withdrawing but mesomerically electron donating substituents on phenyl group is/are required for high activity. On the other hand, only two isatins derivatives (**19** and **20**) showed promising activity with MIC 3.12 and 0.39 μg/mL, respectively. The promising potency of **20** is of interest and reveals the detrimental effect of *N*-substituent of isatin on activity. Surprisingly, introducing trifluoromethoxy or sulfonate at 5-position of isatin or *N*-(*m*-methoxybenzyl) drastically decreased the activity which can be accounted for by either decreasing the solubility (these compounds are poorly soluble in common solvents including DMSO), or steric clash at the binding site.

Activity against dormant forms (nutrient starvation model)

Compounds which showed MIC ≤1.56 μg/mL (**4, 5, 12** and **20**), along with the standard drugs isoniazid, rifampicin and moxifloxacin, were evaluated for their potency against dormant forms of mycobacterium by nutrient starvation model at 10 μg/mL concentration (Betts et al. 2002; De Man 1983). Among the compounds tested compound **20** showed 2.4 log reduction in bacterial count which is comparable to the activity of the tested standard drugs (Fig. 2). Meanwhile, compound **4** was found to be equally efficacious as isoniazid and rifampicin but less potent when compared to moxifloxacin.

Table 1 Anti-mycobacterial activity of compounds **3-21** against *M. tuberculosis* H37Rv strain (ATCC-27294), cytotoxicity and selectivity index (SI)

Compd. no.	Activity MIC[a] (μg/mL)	Cytotoxicity HEK 293 at 50 μg/mL[a] (% inhibition)	Selectivity index
3	12.5	23.45	>4
4	1.56	28.97	>32
5	1.56	34.0	>32
6	12.5	30.9	>4
7	3.12	27.8	>15
8	6.25	30.9	>8
9	12.5	34.56	>4
10	3.12	22.68	>15
11	12.5	31.23	>4
12	1.56	25.56	>32
13	3.12	36.75	>15
14	25	Not tested	–
15	6.25	40.23	>8
16	12.5	27.89	>4
17	>25	Not tested	–
18	>25	Not tested	–
19	3.12	40.78	>15
20	0.39	42.31	>128
21	>25	Not tested	–
PAS	5	ND[b]	–
Isoniazid	0.06	21.78	>833
Rifampicin	0.39	18.12	>128
Ethambutol	3.13	16.90	>15

[a] Values are means of three experiments

[b] Not determined (no inhibition at the tested dose)

Cytotoxicity

The in vitro cytotoxicity for analogues with MIC ≤12.5 μg/mL was assessed using 3-(4,5-dimethylthiazol-2-yl)-2,5-diphenyltetrazolium bromide (MTT) assay (Bézivin et al. 2003; Sykes et al. 2012) against Human Embryonic Kidney (HEK-293T) cells at 50 μg/mL concentration. The percentage inhibition is reported in Table 1. The ratio between in vitro cytotoxicity and *antimycobacterial* activity (MIC in μg/mL) determines the selectivity index (SI). The most promising antitubercular compounds **4**, **5**, **12**, **13**, **19** and **20** exhibited selectivity index >10, revealing good safety margin for the active compounds.

Molecular modeling

HypoGen algorithm as implemented in Discovery Studio 4.1 package (Accelrys, San Diego, CA) was used for the generation of a three-dimensional (3D) pharmacophore

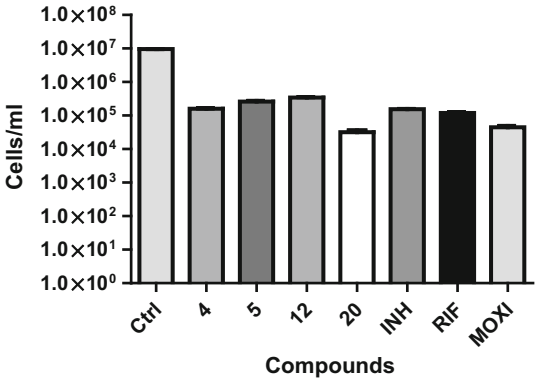

Fig. 2 Activity of compounds (**4**, **5**, **12** and **20**) against nutrient starved MTB model. Bacterial count estimation (Mean ± SD, n = 3) for control and treated groups conducted by using MPN (most probable number) assay. The statistical significance ($p < 0.0001$) with respect to control has been analyzed by Two-way ANOVA using GraphPad Prism Software

model for the 19 (**3**–**21**) tested compounds. In the current study the number of the training set compound (19 derivatives) as well as their biological activity span was optimal for HypoGen pharmacophore generation. The process starts with the generation of low-energy conformations of each ligand in the training set followed by the generation of 10 hypotheses based on HypoGen algorithm (Table 2).

Table 2 Characteristics for the 10 models generated by HypoGen module of catalyst

Model	Total Cost	RMS	Correlation (*r*)
Hypo1	82.1	1.02	0.89
Hypo2	85.1	1.13	0.82
Hypo3	87.1	1.29	0.78
Hypo4	88.3	1.41	0.77
Hypo5	88.6	1.51	0.72
Hypo6	89.4	1.50	0.67
Hypo7	90.1	1.58	0.67
Hypo8	90.3	1.59	0.68
Hypo9	91.5	1.56	0.62
Hypo10	93.8	1.59	0.64

The quality of Hypo1 was tested in terms of fixed cost, null cost and total cost (17). The total cost for each pharmacophore model is the summation of the three cost components; error (E), weight (W), and configuration (C)) multiplied by a coefficient. The fixed cost is the simplest model that fits the data perfectly, while the null cost represents the cost of a hypothesis with no features that estimates every activity to be the average activity. Accordingly, there should be a large difference between the fixed cost and null cost for a pharmocophore of high prediction power. In addition, the total cost of the model should be close to the fixed cost. In case of Hypo1, the difference between the fixed cost (74.1) and the null cost (119.7) is 45.6 which imply a 75–90% probability for correlating the experimental and predicted activity data. Moreover, the total cost for Hypo1 is 82.1 which is close to the fixed cost (74.1) for the hypothesis calculations.

Analysis of the highest ranked pharmacophore shows a model of four features; one hydrogen-bond acceptor (HBA), two aromatic ring features (RA) and a hydrophobic feature (HB) in addition to a "shape inclusion" boundary (Fig. 3).

Mapping of the synthesized active compounds into Hypo1 (Fig. 4) shows similar alignment with the calculated pharmacophoric features with the exception of compounds **4** and **20** which show slightly different orientation. For the majority of the compounds the two aromatic ring features of Hypo1 are mapped into the triazole ring and its C-4 phenyl substituent. The C-2 hydroxyl group of the middle phenyl ring fits well into the hydrogen bond acceptor feature of Hypo1. Finally, the terminal aromatic moiety (either phenyl or indoline rings) maps into the hydrophobic feature of Hypo1. Fitting of the synthesized active compounds into Hypo1 shows similar alignment into the pharmacophore

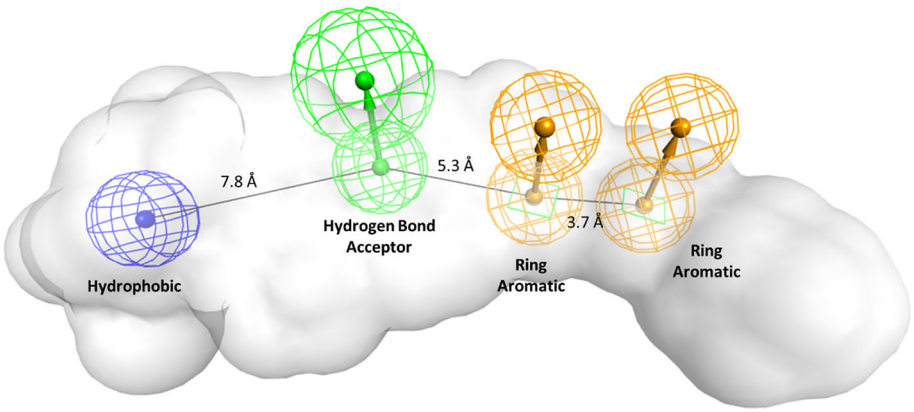

Fig. 3 Spatial arrangements of the structural features for the highest ranked HypoGen model (Hypo1) showing inter-feature distances

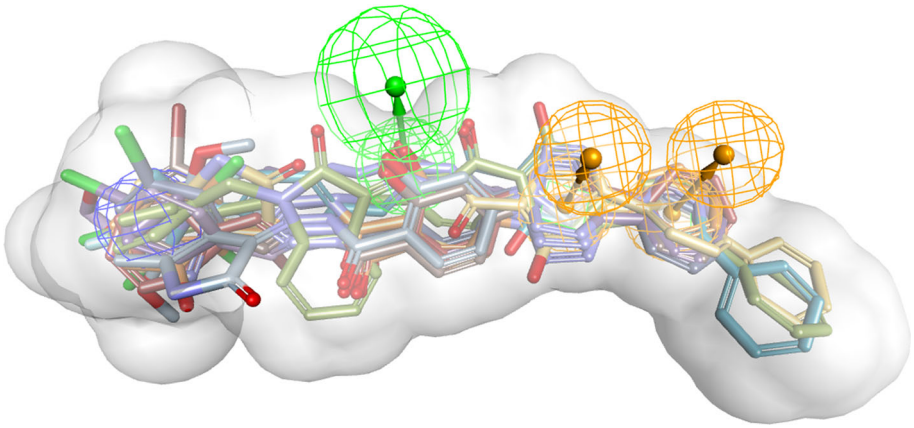

Fig. 4 Active compounds mapped into Hypo1. Model features are colour coded according to Fig. 1

Table 3 Fit values and experimental and predicted activities of the compounds (**3**–**21**)

Compd. no.	Fit value	Activity MIC (μg/mL)	
		Predicted	Experimental
3	6.4	18.586	12.5
4	8.4	1.74183	1.56
5	8.2	2.96206	1.56
6	7.2	7.38495	12.5
7	7.8	4.4691	3.125
8	7.6	4.93569	6.25
9	7.4	10.2701	12.5
10	7.7	2.10814	3.125
11	7.7	6.36325	12.5
12	8.1	2.74376	1.56
13	7.9	3.648	3.125
14	6.5	17.8806	25
15	7.8	3.88851	6.25
16	6.9	13.1027	12.5
17	5.3	43.7326	>25
18	5.1	31.8313	>25
19	7.5	4.63261	3.125
20	8.67	0.931036	0.39
21	6.8	16.76334	>25

features (Fig. 4) as well as good agreement between predicted and observed activity (Table 3, $R = 0.89$).

The most active compound **20** together with compound **4** are showing different orientation while the triazole and the hydroxyphenyl ring map nicely into the two aromatic ring features of Hypo1 (compound **20**, Fig. 5). In this case, the hydrogen bond acceptor feature maps into the N2 of the hydrazine moiety and the hydrophobic feature fits into the terminal phenyl ring similarly to other active compounds. Interestingly, the terminal phenyl ring for these two molecules (**4** and **20**) occupy a hypothetical sub-pocket that is vacant for all other molecules. This may partially explain the high activity of analogue **20** (MIC = 0.39 μg/mL).While it was not possible to explain the observed low activity for compounds **17**, **18** and **21** by simple SAR analysis, mapping of these compounds into Hypo1 shows unfavorable orientation of the C-5 substituents outside the shape inclusion feature (Fig. 6). Moreover, calculating the possible forbidden areas at the receptor side confirmed the orientation of the trifluromethoxy and the sulfonate groups (for **17** and **18** respectively) so that they fit into two "excluded volumes" features (grey maps, Fig. 6). Unfortunately, the model was not able to explain the low activity for compound **21**.

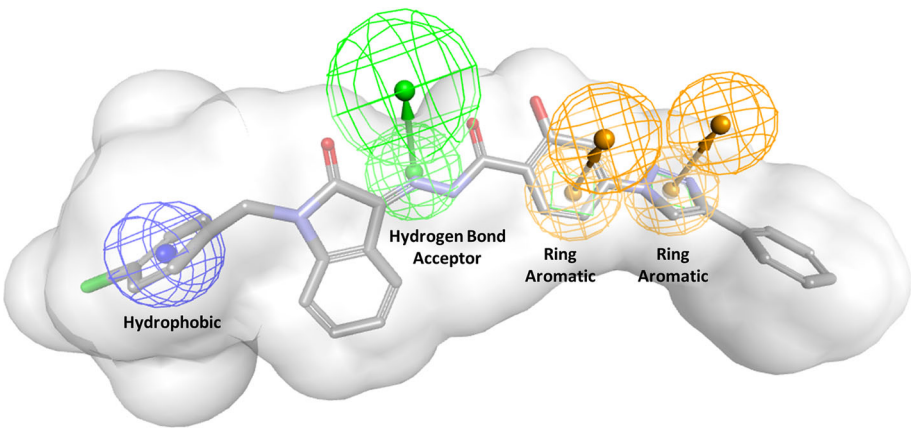

Fig. 5 Mapping of the most active compound (**20**) into Hypo1

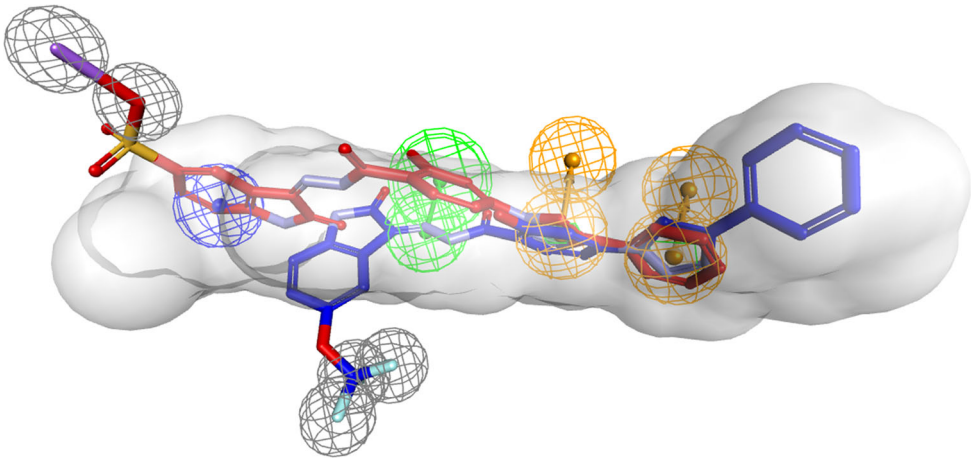

Fig. 6 Mapping of the inactive compounds (**17** and **18**) into Hypo1

Conclusion

Reported here is the synthesis and in vitro antituberculous activities of new 4-phenyl-1*H*-1,2,3-triazol-1-ylsalicylhydrazones. The synthesis was achieved using the inexpensive, commercially available and clinically used PAS. Among the derivatives studied, compound **20** showed remarkably high potency and selectivity index. Moreover, **20** showed 2.4 log reduction in bacterial count of dormant forms of mycobacterium which is comparable with the standard drugs moxifloxacin, isoniazid, rifampicin. 3D-QSAR pharmacophore model was generated and used to evaluate the observed activity. The results demonstrate the potential utility of compound **20** as antitubercular lead compound for further development and mechanistic studies.

Acknowledgement This work was supported by Faculty of Pharmacy, Assiut University.

Compliance with ethical standards

Conflicts of interest The authors declare no conflict of interest.

References

Abdel-Alim AM, El-Shorbagi AN, Abdel-Moty SG, Abdel-Allah HHM (2005) Synthesis and anti-inflammatory testing of some new compounds incorporating 5-aminosalicylic acid (5-ASA) as potential prodrugs. Arch Pharm Res 28:637–647

Abdu-Allah HHM, Abdel-Alim AM, Abdel-Moty SG, El-Shorbagi AA (2005) Synthesis of trigonelline and nicotinamide linked prodrugs of 5-aminosalicylic acid (5-ASA) with analgesic and anti-inflammatory effects. Bull Pharm Sci Assiut Univ 28:237–253

Abdu-Allah HHM, El-Shorbagi ANA, Abdel-Moty SG, El-Awady R, Abdel- Alim AM (2016a) 5-Aminosalyclic acid (5-ASA): a unique anti-inflammatory salicylate. Med Chem (Los Angeles) 6:306–315

Abdu-Allah HHM, Abdel-Moty SG, El-Awady R, El-Shorbagi AN (2016b) Design and synthesis of novel 5-aminosalicylate (5-ASA)-4-thiazolinone hybrid derivatives with promising antiproliferative activity. Bioorg Med Chem Lett 26:1647–1650

Aboul-Fadl T, Bin-Jubair FA, Aboul-Wafa O (2010) Schiff bases of indoline-2,3-dione (isatin) derivatives and nalidixic acid carbohydrazide, synthesis, antitubercular activity and pharmacophoric model building. Eur J Med Chem 45:4578–4586

Aboul-Fadl T, Abdel-Aziz HA, Abdel-Hamid MK, Elsaman T, Thanassi J, Pucci MJ (2011) Schiff bases of indoline-2,3-dione: potential novel inhibitors of *Mycobacterium tuberculosis* (Mtb) DNA gyrase. Molecules 16:7864–7879

Betts JC, Lukey PT, Robb LC, McAdam RA, Duncan K (2002) Evaluation of a nutrient starvation model of Mycobacterium tuberculosis persistence by gene and protein expression profiling. Mol Microbiol 43:717–731

Bézivin C, Tomasi S, Lohézic-Le Dévéhat F, Boustie J (2003) Cytotoxic activity of some lichen extracts on murine and human cancer cell lines. Phytomedicine 10:499–503

De Man JC (1983) MPN tables, corrected. Appl Microbiol Biotechnol 17:301–305

Debnath AK (2002) Pharmacophore mapping of a series of 2,4-diamino-5-deazapteridine inhibitors of Mycobacterium avium complex dihydrofolate reductase. J Med Chem 45:41–53

Emmadi NR, Bingi C, Kotapalli SS, Ummanni R, Nanubolu JB, Atmakur K (2015) Synthesis and evaluation of novel fluorinated pyrazolo-1,2,3-triazole hybrids as antimycobacterial agents. Bioorg Med Chem Lett 25:2918–2922

Evans BE, Rittle KE, Bock MG, DiPardo RM, Freidinger RM, Whitter WL, Lundell GF, Veber DF, Anderson PS, Chang RS (1988) Methods for drug discovery: development of potent, selective, orally effective cholecystokinin antagonists. J Med Chem 31:2235–2246

Franzblau SG, Witzig RS, McLaughlin JC, Torres P, Madico G, Hernandez A, Degnan MT, Cook MB, Quenzer VK, Ferguson RM, Gilman RH (1998) Rapid, low-technology MIC determination with clinical Mycobacterium tuberculosis isolates by using the microplate Alamar Blue assay. J Clin Microbiol 36:362–366

Gano KW, Monbouquette HG, Myles DC (2001) An efficient synthesis of a class of heterobifunctional photo-reactive crosslinkers, labels, and probes. Tetrahedron Lett 42:2249–2251

Humma L (1996) Prevention and treatment of drug-resistant tuberculosis. Am J Health-Syst Pharm 53:2291–2298

Jordão AK, Sathler PC, Ferreira VF, Campos VR, de Souza MC, Castro HC, Lannes A, Lourenco A, Rodrigues CR, Bello ML, Lourenco MC, Carvalho GS, Almeida MC, Cunha AC (2011) Synthesis, antitubercular activity, and SAR study of

N-substituted-phenylamino-5-methyl-1H-1,2,3-triazolo-4-carbohydrazides. Bioorg Med Chem 19:5605–5611

Menendez C, Chollet A, Rodriguez F, Inard C, Pasca MR, Lherbet C, Baltas M (2012) Chemical synthesis and biological evaluation of triazole derivatives as inhibitors of InhA and antituberculosis agents. Eur J Med Chem 52:275–283

Minato Y, Thiede JM, Kordus SL, McKlveen EJ, Turman BJ, Baughn AD (2015) Mycobacterium tuberculosis folate metabolism and the mechanistic basis for para-aminosalicylic acid susceptibility and resistance. Antimicrob Agents Chemother 59:5097–5106

Patole J, Shingnapurkar D, Padhyea S, Ratledge C (2006) Schiff base conjugates of p-aminosalicylic acid as antimycobacterial agents. Bioorg Med Chem Lett 16:1514–1517

Pavan FR, Maia PIDS, Leite SR, Deflon VM, Batista AA, Sato DN, Franzblau SG, Leite CQ (2010) Thiosemicarbazones, semicarbazones, dithiocarbazates and hydrazide/hydrazones: anti-Mycobacterium tuberculosis activity and cytotoxicity. Eur J Med Chem 45:1898–1905

Peloquin C, Berring S, Huitt G, Childs J, Singleton M, James G (1999) Once-daily and twice- daily dosing of p-aminosalicylic acid granules. Am J Respir Crit Care Med 159:932–934

Rengarajan J, Sassetti C, Naroditskaya V, Sloutsky A, Bloom BR, Rubin EJ (2004) The folate pathway is a target for resistance to the drug para-aminosalicylic acid (PAS) in mycobacteria. Mol Microbiol 53:275–282

Shanmugavelan P, Nagarajan S, Sathishkumar M, Ponnuswamy A, Yogeeswari P, Sriram D (2011) Efficient synthesis and in vitro antitubercular activity of 1,2,3-triazoles as inhibitors of *Mycobacterium tuberculosis*. Bioorg Med Chem Lett 21:7273–7276

Sriram D, Yogeeswari P, Meena K (2006) Synthesis, anti-HIV and antitubercular activities of isatin derivatives. Pharmazie 61:274–277

Suman P, Dayakar C, Rajkumar K, Yashwanth B, Yogeeswari P, Sriram D, Rao JV, Raju BC (2015) Synthesis and anti-mycobacterial activity of 2-chloronicotinaldehydes based novel 1H-1,2,3-triazolylbenzohydrazides. Bioorg Med Chem Lett 25:2390–2394

Sykes ML, Baell JB, Kaiser M, Chatelain E, Moawad SR, Ganame D, Ioset JR, Avery VM (2012) Identification of compounds with anti-proliferative activity against Trypanosoma brucei brucei strain 427 by a whole cell viability based HTS campaign. PLoS Negl Trop Dis 6:e1896

Vavříková E, Polanc S, Kočevar M, Košmrlj J, Horváti K, Bosze S, Stolaříková J, Imramovský A, Vinšová J (2011) New series of isoniazid hydrazones linked with electron-withdrawing substituents. Eur J Med Chem 46:5902–5909

Verma A, Yadav MR, Giridhar R, Prajapati N, Tripathi AC, Saraf SK (2013) Nitrogen containing privileged structures and their solid phase combinatorial synthesis. Comb Chem High Throughput Screen 16:345–393

World Health Organization (WHO) (2015) Global Tuberculosis Report. http://www.who.int/tb/publications/global_report/gtbr14_main_text.pdf?ua=1

Zumla A, Nahid P, Cole ST (2013) Advances in the development of new tuberculosis drugs and treatment regimens. Nat Rev Drug Discov 12:388–404